

Dipped adcluster model for chemisorptions and catalytic reactions on a metal surface: Image force correction and applications to Pd-O₂ adclusters

Hiroshi Nakatsuji, Hiromi Nakai, and Yoshifumi Fukunishi

Department of Synthetic Chemistry, Faculty of Engineering, Kyoto University, Kyoto 606, Japan

(Received 31 December 1990; accepted 25 March 1991)

Electrostatic term in the dipped adcluster model proposed previously is estimated by the method of image force. This is superior to the previous one which overestimates the electrostatic correction. The refined method is applied to the Pd-O₂ adcluster dipped onto a free electron bath of the solid metal, the same system as reported previously. In addition to the highest spin coupling, the paired spin coupling is also applied. The former leads to a one-electron transfer and the latter a partial number (0.25) of electron transfer from a bulk metal into an adcluster. The geometry and the vibrational frequencies of the admolecule are not much affected by the electrostatic term, though the heat of adsorption is.

I. INTRODUCTION

Dipped adcluster model (DAM)¹ has been proposed as a theoretical model for studying chemisorptions and surface reactions which involve electron transfer between an admolecule and a surface. It was proposed since the conventional cluster model neglects the effect of a bulk metal. The "adcluster," a combined system of an admolecule and a cluster, is dipped onto the electron "bath" of a solid metal and an equilibrium is established for electron and/or spin transfers between them. While all the electrons transferred into the admolecule must be supplied by the cluster alone in the conventional cluster model, some of the electrons are supplied from the electron bath of the bulk metal in DAM. In particular, the number of electrons, n , transferred from (or to) the bulk metal may be a noninteger in DAM, since it deals with a partial system. It has been shown that the electron transfer between the adcluster and the bulk metal is important for the stabilization of an admolecule on a metal surface.

When an admolecule is charged on a metal surface, the electrostatic interaction between them should be important. In the previous paper,¹ the electrostatic energy was estimated from the Coulombic interaction between the charges on the adcluster and the holes produced in the bulk metal. However, this model was somewhat unnatural since it does not satisfy classical Poisson equation. We propose here a more natural estimation of the electrostatic energy on the basis of the image force on a metal surface. This improves an overestimation of the electrostatic term. The refined method is applied to the Pd-O₂ system with the use of the paired spin coupling as well as the highest spin coupling adopted previously.

Spectroscopic studies have revealed the existence of four molecular oxygen species on a Pd surface, namely, physisorbed (O₂), superoxo (O₂⁻), peroxy-I, and peroxy-II (O₂²⁻) species.²⁻⁴ The O-O stretching frequencies of these four species are observed at 1585, 1035, 850, and 650 cm⁻¹, respectively.²

The physisorbed oxygen is observed after the oxygen saturation on a metal surface, and its O-O vibrational frequency is observed at 1585 cm⁻¹ which is almost the same as that of a free oxygen molecule, 1580 cm⁻¹. An isolated

PdO₂ molecule is also observed at low temperature in an argon matrix and the O-O vibrational frequency is measured at 1024 cm⁻¹.⁵ On the theoretical side, however, there are no studies for molecular adsorptions of O₂ on a Pd surface, except for the *atomic* oxygen adsorption on a Pd surface,⁶ though there are some studies for O₂ adsorptions on the other transition-metal surfaces.⁷⁻¹⁶

In this study, we examine the end-on adsorption of an O₂ molecule on a Pd surface and show an existence of the superoxo species. We show that the conventional cluster model is unable to describe the end-on adsorption, though the DAM certainly describes. We also show that a linear PdO₂ molecule does not exist in an isolated form. For the side-on adsorption of O₂ on a Pd surface, a separate study is being done in our laboratory.¹⁷

A preliminary result of the application of DAM to the O₂ chemisorption on an Ag surface has recently been published.¹⁵ We have shown the existence of the superoxo, peroxy, and dissociative species. The effects of electron transfer, electrostatic interactions, and electron correlations have been shown to be important. Such study has become possible by combining DAM with the SAC (symmetry adapted cluster)¹⁸ and SAC-CI¹⁹ methods developed in our laboratory.

II. ELECTROSTATIC IMAGE FORCE

In DAM, the total energy of the system is given by

$$E = E^{(0)} + E^{(1)} \quad (1)$$

where $E^{(0)}$ is the energy of the adcluster alone and $E^{(1)}$ the energy of the electrostatic interaction between the adcluster and the bulk metal. For $E^{(0)}$, the molecular orbital model of the dipped adcluster was proposed and for $E^{(1)}$, the following two estimates were proposed:

$$E^{(1)} = - \sum_k \lambda_k \left\langle \psi_k \left| \sum_R g_R / r_R \right| \psi_k \right\rangle + \sum_A \sum_R Z_A g_R / R_{AR} + \sum_{R>S} g_R g_S / R_{RS} \quad (2)$$

and

$$E^{(1)} = \sum_A \sum_R g_A g_R / R_{AR} + \sum_{R>S} g_R g_S / R_{RS}, \quad (3)$$

where A runs over the atoms of the adcluster, R, S over the solid metal atoms, and λ_k is the occupation number of the MO ψ_k . Equations (2) and (3) mean that the electrostatic interaction is taken into account, respectively, before and after solving the molecular orbitals of the dipped adcluster. Test calculations have shown that Eq. (3) is a good approximation of Eq. (2).

In the previous paper, the gross charge g_R were distributed over the atoms R of the solid which are the nearest neighbors to the metal atoms of the adcluster. However, this model does not stand with the classical Poisson equation for the metal. We consider here the electrostatic correction through the image force on a metal surface.

When an adatom A at the position \mathbf{a} has a charge q , it induces an opposite charge on a metal surface. At point \mathbf{x} ($x, y, 0$) of the surface, the induced charge density is given by²⁰

$$\sigma(\mathbf{x}) = -\frac{q|\mathbf{a} - \mathbf{a}'|}{4\pi|\mathbf{a} - \mathbf{x}|^3}, \quad (4)$$

where \mathbf{a}' is the positional vector of the mirror image of the adatom A . The electrostatic interaction between the charge q and the hole $\sigma(\mathbf{x})$ sums up to the well-known image force given by

$$\mathbf{F}_{if} = \int \int_{xy}^{\text{surface}} \frac{\sigma(\mathbf{x})q}{|\mathbf{a} - \mathbf{x}|^3} (\mathbf{a} - \mathbf{x}) dx dy = \frac{q^2(\mathbf{a}' - \mathbf{a})}{|\mathbf{a} - \mathbf{a}'|^3}, \quad (5)$$

and the stabilization energy is given by

$$E_{if} = \int \int_{xy}^{\text{surface}} \frac{\sigma(\mathbf{x})q}{2|\mathbf{a} - \mathbf{x}|} dx dy = -\frac{q^2}{2|\mathbf{a}' - \mathbf{a}|}, \quad (6)$$

where the factor 2 in the denominator is due to the integration over the half space.

When the energy $E^{(0)}$ of the adcluster alone is calculated by an *ab initio* method, the electrostatic interaction within the adcluster is already included. Therefore, the electrostatic term $E^{(1)}$ is estimated, as illustrated in Fig. 1, by integrating the electrostatic interaction between the charge q and the hole $\sigma(\mathbf{x})$ at the point \mathbf{x} outside the cluster region of the surface. In practice, the energy $E^{(1)}$ is calculated by subtracting from E_{if} the electrostatic energy (E_{in}) for $\sigma(\mathbf{x})$ inside the cluster region, that is,

$$E^{(1)} = E_{if} - E_{in}. \quad (7)$$

As scheched in Fig. 1, the cluster region of the surface is estimated by the van der Waals radius of the metal atom, and the Mulliken's atomic charge is used for q .

When plural charges q_i are placed on the atoms A_i of a molecule or a supermolecule, the charge density $\sigma(\mathbf{x})$ induced on the surface is given by the Poisson equation as a simple summation of the individual contributions,

$$\sigma(\mathbf{x}) = \sum_i \sigma_i(\mathbf{x}) = -\sum_i \frac{q_i |\mathbf{a}_i - \mathbf{a}'_i|}{4\pi |\mathbf{a}_i - \mathbf{x}|^3}, \quad (8)$$

where \mathbf{a}_i is the positional vector of the atom A_i , \mathbf{a}'_i that of the mirror image. The image force acting on the atom A_i is given by

side view

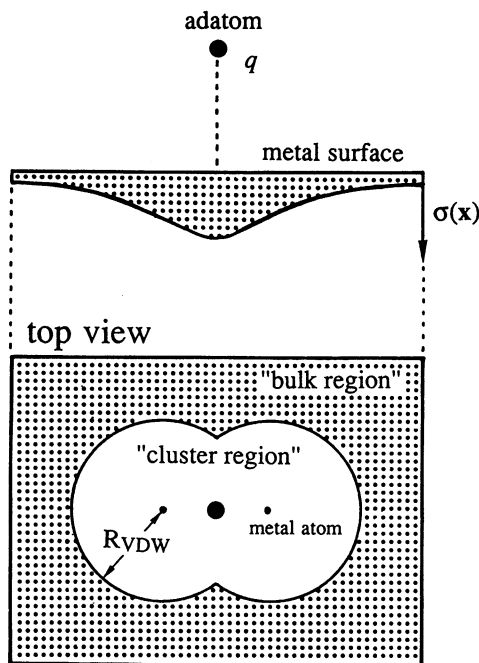


FIG. 1. Schematic representation of the adatom and the induced charge density on the surface. Cluster region is estimated from the van der Waals radius of the metal atom.

$$\mathbf{F}_{if,i} = \sum_j \frac{q_i q_j (\mathbf{a}'_j - \mathbf{a}_i)}{|\mathbf{a}_i - \mathbf{a}'_j|^3}, \quad (9)$$

and the total image force energy by

$$E_{if} = -\sum_i \sum_j \frac{q_i q_j}{2|\mathbf{a}_i - \mathbf{a}'_j|}. \quad (10)$$

The electrostatic term $E^{(1)}$ is calculated similarly by Eq. (7).

The estimation of the electrostatic energy may be done before or after MO calculations. In principle, the effect should be included before MO calculations because then, we can include the relaxation of the electron cloud of the adcluster in the electrostatic field of the surface. Since q_i and $\sigma(\mathbf{x})$ depends on each other, the calculations are done iteratively. We have shown in the previous paper¹ that these two methods using Eqs. (2) and (3) give very similar results. Therefore, we here calculate the image force correction with Eq. (7) after MO calculations.

A difference from the previous treatment is that the electrostatic term $E^{(1)}$ does not necessarily vanish even in the case of $n = 0.0$, i.e., no electron transfer between the adcluster and the bulk metal, though in the previous treatment¹ $E^{(1)}$ vanishes identically when $n = 0.0$.

III. PALLADIUM-O₂ SYSTEM

The dipped adcluster model is applied to the palladium-O₂ system, representing a palladium surface by a single Pd atom. The adcluster is taken as a linear Pd-O-O system. This is the same system as reported previously.¹ We adopt here two different ways of spin coupling for the electrons in

the active MOs. One is the highest (or parallel) spin coupling and the other the paired spin coupling.¹ These are two extreme models of the spin couplings of the electrons in the active MOs. The former gives lower energy than the latter as the energy of the adcluster alone. The former was adopted in the previous calculations, but the latter was not since the electrostatic term $E^{(1)}$ was unballancingly large in comparison with the energy of the adcluster alone $E^{(0)}$. In the present estimate of the electrostatic term, both coupling models give reasonable results.

A. Highest spin coupling

In this coupling scheme, the present result is different from the previous one only in the electrostatic term $E^{(1)}$. The energy $E^{(0)}$ and the electronic structure of the adcluster are entirely the same as the previous ones. The energy E of the system is calculated as a function of n , the number of electrons transferred into the adcluster from the solid. Since the π^* orbitals of O_2 are already singly occupied by the two α -spin electrons in the ${}^3\Sigma_g^-$ state, $n/2$ β -spin electron is added to each of the degenerate π^* orbitals.

Figure 2 is a display of the $E(n)$ curves, calculated as a function of n , for different O–O distances, R_{O-O} . The curves are upper convex and the curvature is discontinuous at $n = 0.0$ and $n = 1.0$. At $n = 0.0$, $R_{O-O} = R_{eq}$ is most stable, but at $n = 1.0$, $R_{O-O} = 1.40 \text{ \AA}$ is most stable. The tangent of the curve for $R_{O-O} = R_{eq}$ does not coincide with the experi-

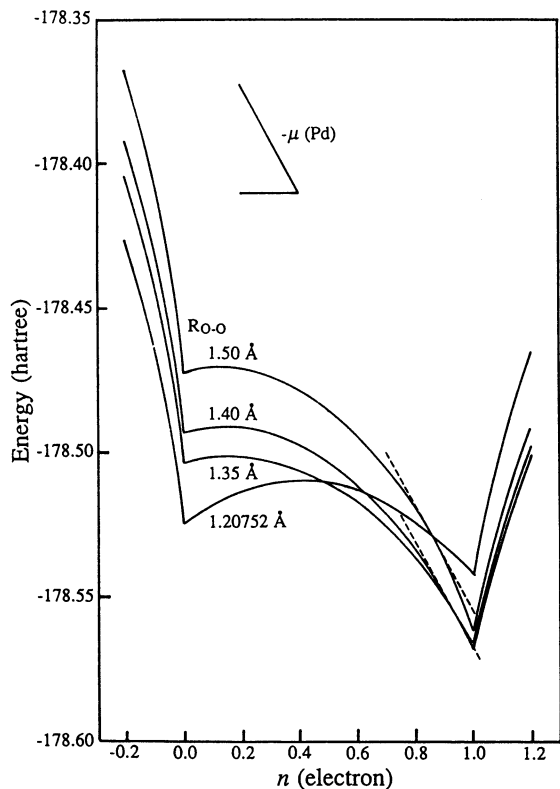


FIG. 2. $E(n)$ curves for the Pd– O_2 – O_2 system in the highest spin coupling model with the O–O distances of 1.207 52, 1.35, 1.40, and 1.50 Å and the Pd– O_2 distance fixed at 2.00 Å.

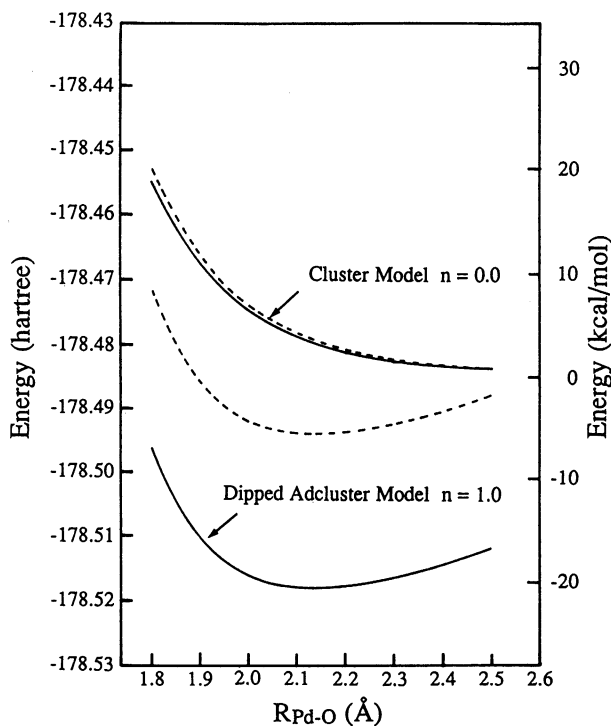


FIG. 3. Potential energy curves for the end-on approach of the O_2 molecule onto palladium calculated by the highest spin coupling. The O–O length is fixed at 1.207 52 Å (equilibrium length of the free O_2) for the upper one and at 1.35 Å for the lower one. Broken and solid lines are calculated, respectively, without and with the electrostatic energies $E^{(1)}$. The upper broken line with $n = 0.0$ corresponds to the cluster model. The energy scale on the right-hand side is in kcal/mol relative to the free Pd plus O_2 system.

mental chemical potential $-\mu$ of the solid palladium metal (5.12 eV),²¹ though it coincides at $n = 0.85$ in the previous calculation. However, the tangent of the curves for $R_{O-O} = 1.35 \sim 1.50 \text{ \AA}$ coincides with $-\mu$ at $n = 0.8 \sim 1.0$. Therefore, after some barrier, one electron flows from the bulk metal into the adcluster as explained in Ref. 1.

Figure 3 shows the potential energy curve for the end-on approach of the O_2 molecule to the palladium surface. The broken lines are for $E^{(0)}$ alone and the solid lines for $E^{(0)} + E^{(1)}$. The broken and solid curves for $n = 0.0$ nearly overlap each other, since the electrostatic term is very small. The broken curve for $n = 0.0$ corresponds to the cluster model, which results in that the O_2 molecule is not adsorbed onto Pd in contrary to the experiment. This result also shows that a linear PdO_2 molecule does not exist. On the other hand, when the electron transfer from the bulk to the adcluster is admitted, the system becomes stable as O_2 approaches Pd, which is shown by the broken curve of $n = 1.0$. Furthermore, the image force term is also important for stabilizing the system as shown by the solid curve of $n = 1.0$.

The equilibrium Pd–O length and the Pd–O stretching frequency of the adsorbed state are calculated to be 2.15 Å and 338 cm^{-1} , respectively. The frequency of 338 cm^{-1} may be an underestimate since we assumed that the O_2 molecule vibrates as a whole. The experimental value is 485 cm^{-1} for the O_2 molecule on a Pt(111) surface.²² A similar value of

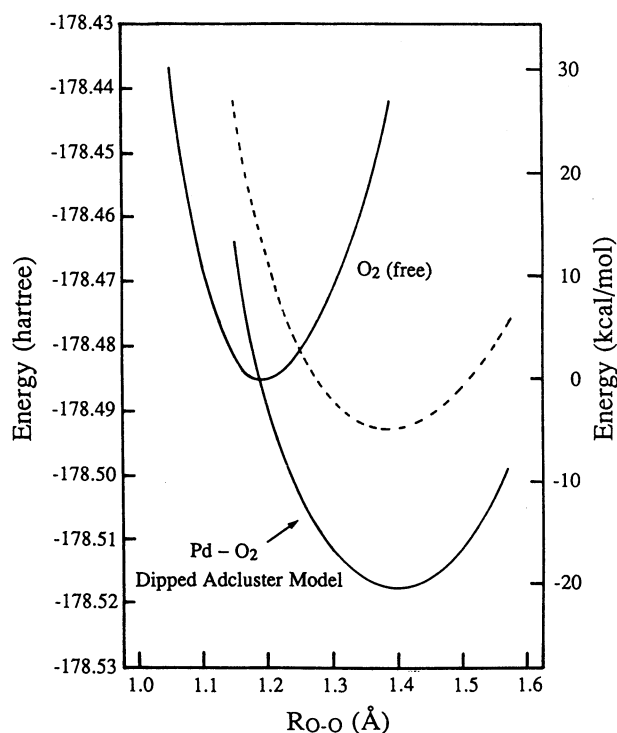


FIG. 4. Potential energy curves for the O-O vibrations of the free O_2 molecule and the adsorbed O_2 molecule on Pd in the dipped adcluster model ($n = 1.0$, highest spin coupling) with the Pd-O distance fixed at 2.00 Å. Broken and solid lines are calculated without and with the electrostatic energies $E^{(1)}$, respectively. The energy scale on the left-hand side is in hartree for the Pd + O_2 system, and the energy scale on the right-hand side is in kcal/mol relative to the free Pd plus O_2 system.

480 cm^{-1} was reported for the Pd-O vibration of the dissociated oxygen on a Pd surface.² The optimized O-O length is 1.40 Å. The adsorption energy is calculated to be 21.9 and 6.4 kcal/mol, respectively, with and without including the image force correction. The molecular adsorption energy by the temperature programmed desorption (TPD) experiment³ is observed at 7.6~12.3 kcal/mol. In the previous study which used Eqs. (2) and (3), the adsorption energy was calculated to be 53.6 kcal/mol, which is too large to

compare with the experimental value. Thus, the present estimation of $E^{(1)}$ is more reasonable than the previous one.

It is noted that the cluster model using one Pd atom fails to describe the end-on adsorption of an O_2 molecule. This failure is mainly due to a limitation of the cluster model. Namely, all the electrons transferred to O_2 must be supplied from the cluster. A larger-size cluster must be used for describing within the cluster model. Then, how large should the size of the cluster be? For example, Upton *et al.* used Ag_{24} cluster for studying O_2 chemisorption on an Ag surface by the GVB and GVB-CI methods.⁹ Geometric and spectroscopic parameters were calculated in good agreement with the available experimental data. However, the adsorption energy relative to the ground states of the cluster and O_2 was calculated to be *negative*, -14.8 kcal/mol. On the other hand, the DAM has been able to give reasonable *positive* adsorption energies for the O_2 adsorptions on an Ag surface with the use of the Ag_2-O_2 and Ag_4-O_2 adclusters.¹⁵ The geometric and spectroscopic properties calculated by DAM have also excellently reproduced the observed values.

Figure 4 shows the calculated potential energy curve for the O-O vibration of O_2 in a gaseous state and in the adsorbed state. The Pd-O distance is fixed at 2.00 Å ($n = 1.0$). The broken line is calculated without $E^{(1)}$ and the solid one with it. The equilibrium O-O length is calculated to be 1.22 and 1.40 Å for the free and adsorbed states, respectively. The experimental value for the former is 1.207 52 Å.¹⁰ The adsorbed O_2 has approximately three electrons in the degenerate π^* orbitals, so that it corresponds to a superoxo species O_2^- . The NEXAFS measurement for the superoxide on the Pt(111) surface has given the O-O bond length of 1.32 ± 0.05 Å,²⁴ which is shorter than our highest spin coupling result. The O-O vibrational frequencies are calculated to be 1707 and 1272 cm^{-1} for the free and adsorbed states, respectively, in comparison with the experimental values of 1580 (Ref. 23) and 1035 (Ref. 2) cm^{-1} , respectively. As is well known, the Hartree-Fock model overestimates the vibrational frequency.

Table I shows the Mulliken's atomic charge and the electrostatic and total energies $E^{(1)}$ and E of the PdO_2 adcluster. When no electron is transferred from the bulk metal,

TABLE I. Mulliken's atomic charge and electrostatic and total energies of the $Pd-O_a-O_b$ adcluster in the highest spin coupling model.^a

n	R_{O-O} (Å)	Mulliken's atomic charge				Electrostatic energy ^b			Total energy ^c
		Pd	O_a	O_b	$O_a + O_b$	E_f	E_m	$E^{(1)}$	$E^{(0)} + E^{(1)}$
0.0	1.207 52	+ 0.093	- 0.120	+ 0.027	- 0.093	- 0.41	- 0.18	- 0.23	- 178.474 65
0.0	1.35	+ 0.169	- 0.140	- 0.029	- 0.169	- 1.09	- 0.39	- 0.70	- 178.452 83
0.0	1.40	+ 0.203	- 0.068	- 0.135	- 0.203	- 1.20	- 0.31	- 0.89	- 178.442 62
0.0	1.50	+ 0.262	- 0.064	- 0.198	- 0.262	- 1.85	- 0.43	- 1.42	- 178.422 04
1.0	1.207 52	- 0.218	- 0.479	- 0.303	- 0.782	- 21.16	- 6.88	- 14.28	- 178.492 07
1.0	1.35	- 0.193	- 0.555	- 0.252	- 0.807	- 23.03	- 7.73	- 15.30	- 178.516 20
1.0	1.40	- 0.180	- 0.584	- 0.236	- 0.820	- 23.98	- 8.14	- 15.84	- 178.517 87
1.0	1.50	- 0.172	- 0.563	- 0.265	- 0.828	- 23.82	- 7.89	- 15.93	- 178.511 51

^a Pd- O_a length is at 2.00 Å.

^b In kcal/mol.

^c In hartree.

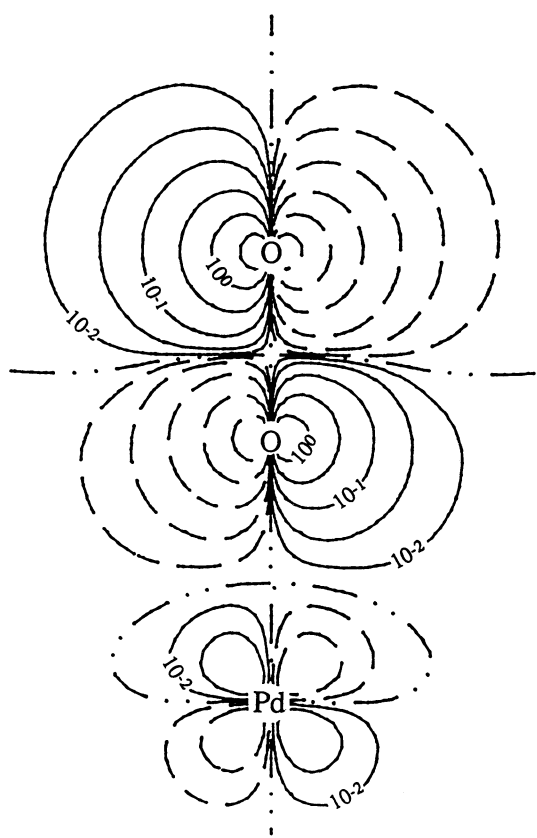


FIG. 5. Contour map of the frontier orbital of the PdO₂ adcluster with $n = 1.0$. The MO is calculated at the Pd–O distance of 2.00 Å and the O–O distance of 1.40 Å. Solid and broken lines correspond to plus and minus signs in the MO. Double dotted line corresponds to the node of the MO. The values of the contours correspond to $10^{0.5}$, 10^0 , $10^{-0.5}$, 10^{-1} , $10^{-1.5}$, and 10^{-2} , respectively.

i.e., $n = 0.0$, the charge of O₂ and therefore the electrostatic term is small. Note that $E^{(1)}$ is nonzero in contrast to the previous case which used Eqs. (2) and (3). At $n = 1.0$, O₂ is charged to about -0.8 and $E^{(1)}$ becomes to $-14 \sim -16$ kcal/mol. While the total electrostatic energy E_{if} is $-21 \sim -24$ kcal/mol, the energy E_{in} is only $-7 \sim -8$ kcal/mol. The ratio of $E^{(1)}/E_{if}$ is about $2/3$, and decreases as the cluster size is taken larger.

The negative charge is larger on O_a than on O_b. A similar polarization of O₂ on an Ag surface has been reported by Broomfield *et al.*¹¹ and Nakatsuji *et al.*¹⁶ Figure 5 illustrates the frontier orbital map, which is related to the reactivity of the adsorbed oxygen species. It consists mainly of the π^* orbitals of O₂ and partly the $4d_{xz}$ (or $4d_{yz}$) orbital of Pd. In contrast to the charge distribution, the frontier orbital is larger at O_b than at O_a, which indicates that the former is more reactive than the latter.

In Table II, we summarize the influence of the electrostatic term $E^{(1)}$ to the adsorption energy and the geometric and spectroscopic parameters of the PdO₂ system. The electrostatic interaction is important for stabilizing the adsorbed O₂ as mentioned before. On the other hand, the bond lengths and force constants calculated with and without $E^{(1)}$ are very similar. This is also seen from Figs. 3 and 4; namely, the potential energy curves with and without $E^{(1)}$ are similar and only shifted. This is because the image force is a long-range force which depends on $1/r$, and the chemical bondings between O–O and Pd–O are mainly described by the short-range forces which depend exponentially like two-center overlap integrals. Thus, the electrostatic term $E^{(1)}$ is essential for describing the energetics of the surface–molecule interaction, but influences to a less extent to the geometric and spectroscopic parameters of the adsorbed molecules.

B. Paired spin coupling

In this section, we show the results of the Pd–O₂ system calculated by the paired spin coupling model, in which the same amounts of α - and β -spin electrons occupy the frontier MO. In the linear Pd–O₂ system, the frontier MOs are mainly composed of the degenerate π^* MOs of O₂. At the separated limit, the triplet state of O₂ has two α - and no β -spin electrons, so that the adsorbed state is not continuously connected to the separated limit without introducing further assumptions. Note however that for adsorptions of closed-shell molecules, this model can give a continuous potential curve between the separated and adsorbed states.

Figure 6 is a display of the $E(n)$ curve, calculated as a function of n . The curves are lower convexes in contrast to the upper ones of Fig. 2. At $n = 0.25$, the tangent of the curve for $R_{O-O} = 1.35$ Å coincides with the chemical potential

TABLE II. Effect of the electrostatic term $E^{(1)}$ on the adsorption energy, geometry, and vibrational frequency of the PdO₂ adcluster in the highest spin coupling model.

	Adsorption energy ^a (kcal/mol)	Bond length (Å)		Vibrational frequency (cm ⁻¹)	
		R_{Pd-O}	R_{O-O}	ω_{Pd-O} ^b	ω_{O-O}
$E^{(0)}$ alone	6.4	2.15	1.39	329	1229
$E^{(0)} + E^{(1)}$	21.9	2.15	1.40	338	1250
Experiment	7.6 ~ 12.3 ^c		1.32 ± 0.05 ^d	485 ^e	1035 ^f

^a Relative to the HF energy of Pd (¹S) + O₂(³Σ_g⁻); -178.48500 hartree.

^b O₂ is assumed to vibrate as a unit.

^c Reference 3.

^d For O₂ on a Pt(111) surface. Reference 24.

^e For O₂ on a Pt(111) surface. Reference 22.

^f Reference 2.

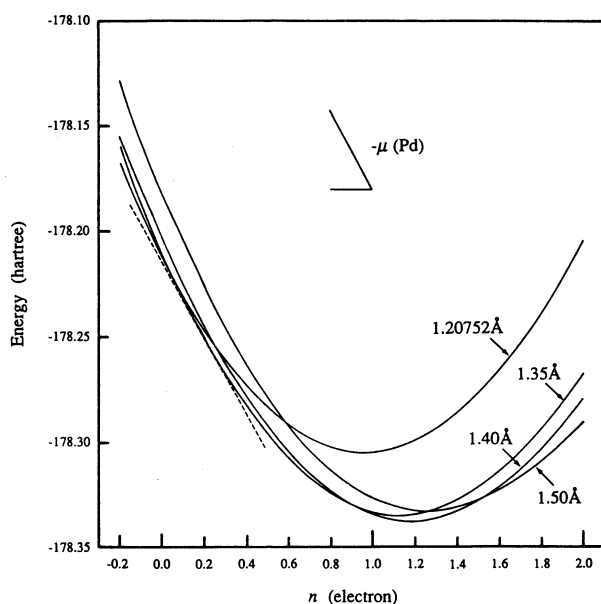


FIG. 6. $E(n)$ curves for the Pd- O_a - O_b system in the paired spin coupling model with the O-O distances of 1.207 52, 1.35, 1.40, and 1.50 Å and the Pd- O_a distance fixed at 2.00 Å.

$-\mu$ of the solid palladium metal (5.12 eV),²¹ and the adcluster is the most stable there in the range of $\partial E/\partial n \leq -\mu$. Therefore, about 0.25 electrons flow into the adcluster from the bulk metal; thus, the adcluster has a noninteger number of electrons. When the chemical potential μ of the metal is regulated, for example, by an external potential, the number of electrons n transferred into the adcluster are regulated. At the limit of $\mu = 0.0$, about 1.15 electrons flow into the adcluster, which corresponds to the minimum of the $E(n)$ curve for $R_{O-O} = 1.40$ Å.

Table III shows the Mulliken's atomic charge and the electrostatic and total energies of the PdO₂ adcluster with $R_{O-O} = 1.35$ Å and $R_{Pd-O} = 2.00$ Å. Though the charge of O₂ increases as n increases, O₂ is charged to -0.43 even at $n = 0.0$, and the image force correction is calculated to be

4.42 kcal/mol. This result differs from that at $n = 0.0$ by the highest spin coupling model; $E^{(1)} = 0.70$ kcal/mol. The negative charge of O_a is larger than that of O_b and the Pd atom is positively charged in the range of $n = 0.0 \sim 0.8$. At $n = 0.25$, the charge of O₂ is -0.55 and that of Pd is $+0.30$. This shows that 0.30 electrons are supplied by the adsorbed Pd atom and 0.25 electrons from the bulk metal. We think it natural that the Pd atom adsorbed by O₂ has positive charge, though this was not the case in the highest spin coupling model.

Figures 7 and 8 show the potential energy curves for the Pd-O and O-O vibrations, respectively, of the Pd-O₂ adcluster with fixed n of 0.25, though of course, the number of electrons n should be optimized as the functions of these distances. Further, the O-O distance is fixed at 1.35 Å in Fig. 7, and the Pd-O distance at 2.00 Å in Fig. 8. These figures correspond to Figs. 3 and 4 for the highest spin coupling model. Broken and solid lines are calculated respectively without and with the image force term $E^{(1)}$.

Table IV shows the calculated geometries and vibrational frequencies of the adsorbed system. They correspond to those of the superoxide species. The influences of $E^{(1)}$ to these parameters are again very small. The bond lengths of the Pd-O and O-O bonds calculated by the paired spin coupling are a little shorter than those by the highest spin coupling, and the force constants are a little larger. The O-O length of 1.31 Å obtained by the paired spin coupling agrees better with the experimental value of 1.32 ± 0.05 Å (Ref. 24) than that obtained by the highest spin coupling. These results imply that both bonds are calculated to be a bit stronger by the paired spin coupling than by the highest spin coupling. It has been shown that the electron repulsion in the active orbital is minimum for the highest spin coupling and maximum for the paired spin coupling.¹ Therefore, it is expected that the MOs in the paired spin coupling is relaxed for reducing the electron repulsion in comparison with the highest spin coupling. This results in the delocalization of the O₂ electrons into Pd and works to strengthen the Pd-O bond. The active MOs are the π antibonding for the O-O bond. The occupation number of these MOs in the paired spin cou-

TABLE III. Mulliken's atomic charge and electrostatic and total energies of the Pd- O_a - O_b adcluster in the paired spin coupling model.^a

n	Mulliken's atomic charge				Electrostatic energy ^b			Total energy ^c
	Pd	O _a	O _b	O _a + O _b	E_f	E_m	$E^{(1)}$	$E^{(0)} + E^{(1)}$
0.0	+ 0.433	- 0.304	- 0.129	- 0.433	- 6.69	- 2.26	- 4.42	- 178.209 02
0.2	+ 0.322	- 0.338	- 0.184	- 0.522	- 9.42	- 3.09	- 6.33	- 178.249 82
0.25	+ 0.301	- 0.349	- 0.202	- 0.551	- 10.45	- 3.40	- 7.05	- 178.259 04
0.4	+ 0.221	- 0.376	- 0.245	- 0.621	- 13.06	- 4.18	- 8.88	- 178.282 82
0.6	+ 0.116	- 0.413	- 0.303	- 0.716	- 17.07	- 5.35	- 11.71	- 178.307 50
0.8	+ 0.008	- 0.449	- 0.359	- 0.808	- 21.53	- 6.67	- 14.86	- 178.324 12
1.0	- 0.101	- 0.484	- 0.416	- 0.899	- 26.46	- 8.11	- 18.35	- 178.332 89
1.2	- 0.211	- 0.518	- 0.471	- 0.989	- 31.77	- 9.64	- 22.13	- 178.333 98
1.4	- 0.323	- 0.550	- 0.527	- 1.077	- 37.38	- 11.24	- 26.14	- 178.327 64

^a Pd- O_a length is at 2.00 Å and O_a - O_b length at 1.35 Å.

^b In kcal/mol.

^c In hartree.

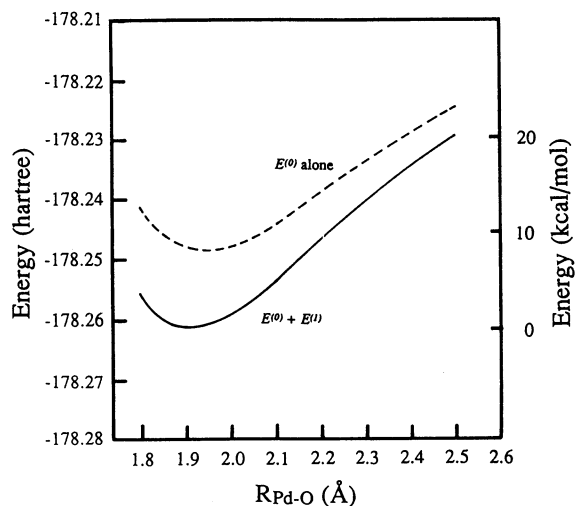


FIG. 7. Potential energy curves for Pd-O vibration calculated by the paired spin coupling. The O-O length is fixed at 1.35 Å. Broken and solid lines are calculated, respectively, without and with the electrostatic energies $E^{(1)}$.

pling (~ 2.25) is smaller than that in the highest spin coupling (~ 3.0), so that the O-O bond is calculated to be stronger in the former than in the latter.

IV. CONCLUDING REMARKS

In the present study, we have proposed the estimation of the electrostatic energy on the basis of the image force on a metal surface. This estimation seems to be superior to the previous one which overestimated the electrostatic correction. The refined method is applied to the Pd-O₂ system with the use of the highest and paired spin couplings. In both spin couplings, the electrostatic term does not affect much on the geometry and the vibrational frequencies of the ad-molecule, though it does for the heat of adsorption.

We have examined the highest (or parallel) and paired

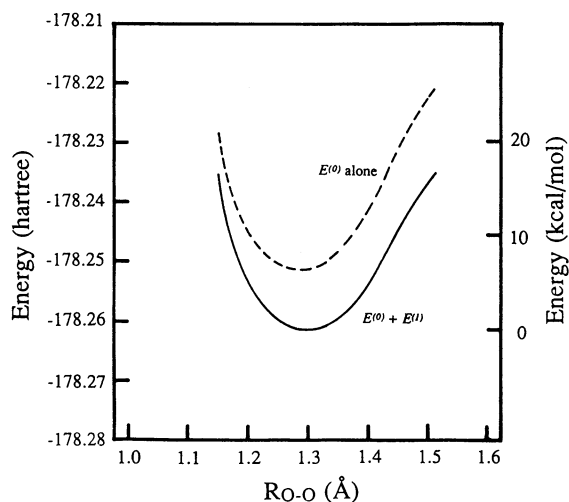


FIG. 8. Potential energy curves for the O-O vibration of the adsorbed O₂ molecule on Pd in the dipped adcluster model ($n = 0.25$, paired spin coupling) with the Pd-O distance fixed at 2.00 Å. Broken and solid lines are calculated without and with the electrostatic energies $E^{(1)}$, respectively.

TABLE IV. Geometry and vibrational frequency of the PdO₂ adcluster calculated by the paired spin coupling model.

	Bond length (Å)		Vibrational frequency (cm ⁻¹)	
	R _{Pd-O}	R _{O-O}	$\omega_{\text{Pd-O}}$ ^a	$\omega_{\text{O-O}}$
$E^{(0)}$ alone	1.96	1.30	389	1259
$E^{(0)} + E^{(1)}$	1.93	1.31	399	1279
Experiment		1.32 ± 0.05 ^b	485 ^c	1035 ^d

^a O₂ is assumed to vibrate as a unit.

^b For O₂ on a Pt(111) surface. Reference 24.

^c For O₂ on a Pt(111) surface. Reference 22.

^d Reference 2.

spin coupling models and the differences are as follows:

(1) The electron repulsion in the active orbital is minimum for the highest spin coupling and maximum for the paired spin coupling. Therefore, the adcluster itself is more stable in the highest spin coupling than in the paired spin coupling.

(2) Two models are very different in the local magnetic property. The adcluster is paramagnetic in the highest spin coupling, but diamagnetic in the paired spin coupling. Since this is an observable property, we expect systematic experiments.

(3) The behaviors of the $E(n)$ curves as a function of n differ from each other for the reason (1) above. The highest spin coupling tends to give an upper convex for the $E(n)$ curve, but the paired one a lower convex. This means that an *integral* number of electrons will transfer into the adcluster in the former model but *nonintegral* number of electrons are transferred in the latter model.

(4) For paramagnetic molecules like O₂ in the $^3\Sigma_g^-$ state, the potential energy curve calculated by the paired spin coupling does not connect with the separated system, though the curve calculated by the highest spin coupling does. For the energy level of chemisorptions of closed-shell molecules, both couplings give connected curves.

(5) When the variational calculation is carried out, the MOs in the paired spin coupling tend to reorganize to relax the electron repulsion in the active MOs in comparison with those in the highest spin coupling.

(6) The Pd-O bond calculated by the paired spin coupling is a little stronger than that by the highest spin coupling since the delocalization of the O₂ electrons is larger in the former for reason (5) above.

(7) The O-O bond of the Pd-O₂ adcluster calculated by the paired spin coupling is a little stronger than that by the highest spin coupling because the number of the occupied electrons in the former is less than that in the latter.

The highest and paired spin couplings are two extreme models. The choice of the models would depend on the nature of the actual systems. The cluster-size dependence in DAM is also an interesting problem to be studied in future. We believe that the size dependence in DAM should be smaller than that in the cluster model. Further, it is evident that electron correlations are very important for chemisorptions and catalytic reactions on a metal surface, since

they involve transition metals and bond breaking and forming processes. We have applied DAM to O₂ chemisorption on an Ag surface,¹⁵ including electron correlations by the SAC/SAC-CI method.^{18,19}

ACKNOWLEDGMENTS

The calculations have been carried out with the FACOM M780 computer at the Data Processing Center of Kyoto University. This study has been partially supported by the Grant-in-Aid for Scientific Research from the Japanese Ministry of Education, Science, and Culture, and by the Kurata Foundation.

¹H. Nakatsuji, *J. Chem. Phys.* **87**, 4995 (1987).

²R. Imbuhl and E. Demuth, *Surf. Sci.* **173**, 395 (1986).

³X. Guo, L. Hanley, and J. T. Yates, Jr., *J. Chem. Phys.* **90**, 5200 (1989); X. Guo, A. Hoffman, and J. T. Yates, Jr., *ibid.* **90**, 5787 (1989); A. Hoffman, X. Guo, J. T. Yates, Jr., J. W. Gadzuk, and C. W. Clark, *ibid.* **90**, 5793 (1989); X. Guo, L. Hanley, and J. T. Yates, Jr., *ibid.* **91**, 7220 (1989).

⁴T. Matsushima, *Surf. Sci.* **157**, 297 (1985).

⁵H. Huber, W. Klotzbucher, G. A. Ozin, and A. Vander Voet, *Can. J. Chem.* **51**, 2722 (1973).

⁶O. Bellezza, M. G. Cattania, A. Gavezzotti, and M. Simonetta, *Chem.*

Phys. Lett. **108**, 425 (1984).

⁷A. Selmani, J. M. Sichel, and D. R. Salahub, *Surf. Sci.* **157**, 208 (1985); A. Selmani, J. Andzelm, and D. R. Salahub, *Int. J. Quantum Chem.* **29**, 829 (1986).

⁸M. L. McKee, *J. Chem. Phys.* **87**, 3143 (1987).

⁹T. H. Upton, P. Stevens, and R. J. Madix, *J. Chem. Phys.* **88**, 3988 (1988).

¹⁰E. A. Carter and W. A. Goddard III, *Surf. Sci.* **209**, 243 (1989).

¹¹K. Broomfield and R. M. Lambert, *Mol. Phys.* **66**, 421 (1989).

¹²P. J. van den Hoek, E. J. Baerends, and R. A. van Santen, *J. Phys. Chem.* **93**, 646 (1989).

¹³I. Panas and P. Siegbahn, *Chem. Phys. Lett.* **153**, 458 (1988); I. Panas, P. Siegbahn, and U. Wahlgren, *J. Chem. Phys.* **90**, 6791 (1989).

¹⁴Y. Mochizuki, U. Nagashima, S. Yamamoto, and H. Kashiwagi, *Chem. Phys. Lett.* **164**, 225 (1989).

¹⁵H. Nakatsuji and H. Nakai, *Chem. Phys. Lett.* **174**, 283 (1990).

¹⁶H. Nakatsuji and H. Nakai (unpublished).

¹⁷H. Nakatsuji and T. Nakao (unpublished).

¹⁸H. Nakatsuji and K. Hirao, *J. Chem. Phys.* **68**, 2035 (1978).

¹⁹H. Nakatsuji, *Chem. Phys. Lett.* **59**, 362 (1978); **67**, 329,334 (1979).

²⁰J. H. Jeans, *The Mathematical Theory of Electricity and Magnetism* (Cambridge University, New York, 1966), Chap. VIII.

²¹H. B. Michaelson, *J. Appl. Phys.* **48**, 4729 (1977).

²²J. L. Gland, B. A. Sexton, and G. B. Fisher, *Surf. Sci.* **95**, 587 (1980).

²³K. P. Huber and G. Herzberg, *Molecular Spectra and Molecular Structure, IV. Constants of Diatomic Molecules* (Van Nostrand Reinhold, New York, 1979).

²⁴D. A. Outka, J. Stohr, W. Jark, P. Stevens, J. Salomons, and R. J. Madix, *Phys. Rev. B* **35**, 4119 (1987).